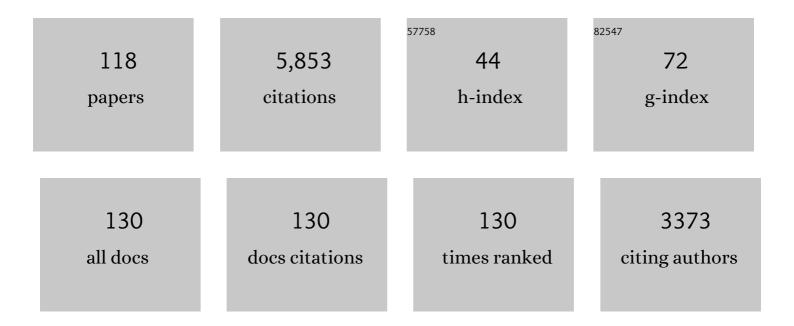
William E Mcclintock

List of Publications by Year in descending order

Source: https://exaly.com/author-pdf/6291926/publications.pdf Version: 2024-02-01



#	Article	IF	CITATIONS
1	Improving the Thermosphere Ionosphere in a Whole Atmosphere Model by Assimilating GOLD Disk Temperatures. Journal of Geophysical Research: Space Physics, 2022, 127, .	2.4	5
2	SOLar-STellar Irradiance Comparison Experiment II (SOLSTICE II): End-of-Mission Validation of the SOLSTICE Technique. Solar Physics, 2022, 297, 1.	2.5	9
3	Sounding Rocket Observation of Nitric Oxide in the Polar Night. Journal of Geophysical Research: Space Physics, 2022, 127, .	2.4	1
4	Laboratory Study of the Cameron Bands, the First Negative Bands, and Fourth Positive Bands in the Middle Ultraviolet 180–280Ânm by Electron Impact Upon CO. Journal of Geophysical Research E: Planets, 2021, 126, .	3.6	7
5	Observation of Postsunset OI 135.6Ânm Radiance Enhancement Over South America by the GOLD Mission. Journal of Geophysical Research: Space Physics, 2021, 126, e2020JA028108.	2.4	28
6	First Comparison of Traveling Atmospheric Disturbances Observed in the Middle Thermosphere by Clobalâ€Scale Observations of the Limb and Disk to Traveling Ionospheric Disturbances Seen in Groundâ€Based Total Electron Content Observations. Journal of Geophysical Research: Space Physics, 2021, 126, e2021JA029248.	2.4	6
7	Investigation of a Neutral "Tongue―Observed by GOLD During the Geomagnetic Storm on May 11, 2019. Journal of Geophysical Research: Space Physics, 2021, 126, e2020JA028817.	2.4	46
8	Variations in Thermosphere Composition and Ionosphere Total Electron Content Under "Geomagnetically Quiet―Conditions at Solarâ€Minimum. Geophysical Research Letters, 2021, 48, e2021GL093300.	4.0	40
9	Response of GOLD Retrieved Thermospheric Temperatures to Geomagnetic Activities of Varying Magnitudes. Geophysical Research Letters, 2021, 48, e2021GL093905.	4.0	18
10	Martian water loss to space enhanced by regional dust storms. Nature Astronomy, 2021, 5, 1036-1042.	10.1	40
11	Impact of GOLD Retrieved Thermospheric Temperatures on a Whole Atmosphere Data Assimilation Model. Journal of Geophysical Research: Space Physics, 2021, 126, e2020JA028646.	2.4	12
12	Thermospheric Composition and Solar EUV Flux From the Global cale Observations of the Limb and Disk (GOLD) Mission. Journal of Geophysical Research: Space Physics, 2021, 126, e2021JA029517.	2.4	26
13	GOES-R Series Solar X-ray and Ultraviolet Irradiance. , 2020, , 233-242.		5
14	The Twoâ€Dimensional Evolution of Thermospheric â~O/N ₂ Response to Weak Geomagnetic Activity During Solarâ€Minimum Observed by GOLD. Geophysical Research Letters, 2020, 47, e2020GL088838.	4.0	59
15	First Clobalâ€Scale Synoptic Imaging of Solar Eclipse Effects in the Thermosphere. Journal of Geophysical Research: Space Physics, 2020, 125, e2020JA027789.	2.4	17
16	First Zonal Drift Velocity Measurement of Equatorial Plasma Bubbles (EPBs) From a Geostationary Orbit Using GOLD Data. Journal of Geophysical Research: Space Physics, 2020, 125, e2020JA028173.	2.4	33
17	Comparison of GOLD Nighttime Measurements With Total Electron Content: Preliminary Results. Journal of Geophysical Research: Space Physics, 2020, 125, e2019JA027767.	2.4	35
18	Neutral Exospheric Temperatures From the GOLD Mission. Journal of Geophysical Research: Space Physics, 2020, 125, e2020JA027814.	2.4	11

#	Article	IF	CITATIONS
19	Daily Variability in the Terrestrial UV Airglow. Atmosphere, 2020, 11, 1046.	2.3	4
20	Variations of Lower Thermospheric FUV Emissions Based on GOLD Observations and GLOW Modeling. Journal of Geophysical Research: Space Physics, 2020, 125, e2020JA027810.	2.4	3
21	Observation of Thermospheric Gravity Waves in the Southern Hemisphere With GOLD. Journal of Geophysical Research: Space Physics, 2020, 125, e2019JA027405.	2.4	8
22	Early Morning Equatorial Ionization Anomaly From GOLD Observations. Journal of Geophysical Research: Space Physics, 2020, 125, e2019JA027487.	2.4	15
23	Globalâ€Scale Observations of the Limb and Disk Mission Implementation: 2. Observations, Data Pipeline, and Level 1 Data Products. Journal of Geophysical Research: Space Physics, 2020, 125, e2020JA027809.	2.4	26
24	First Synoptic Observations of Geomagnetic Storm Effects on the Globalâ€5cale OI 135.6â€nm Dayglow in the Thermosphere by the GOLD Mission. Geophysical Research Letters, 2020, 47, e2019GL085400.	4.0	14
25	A New Data Set of Thermospheric Molecular Oxygen From the Globalâ€scale Observations of the Limb and Disk (GOLD) Mission. Journal of Geophysical Research: Space Physics, 2020, 125, e2020JA027812.	2.4	8
26	New Observations of Largeâ€5cale Waves Coupling With the Ionosphere Made by the GOLD Mission: Quasiâ€16â€Day Wave Signatures in the Fâ€Region OI 135.6â€nm Nightglow During Sudden Stratospheric Warmings. Journal of Geophysical Research: Space Physics, 2020, 125, e2020JA027880.	2.4	24
27	The UV Spectrum of the Lymanâ€Birgeâ€Hopfield Band System of N ₂ Induced by Cascading from Electron Impact. Journal of Geophysical Research: Space Physics, 2020, 125, e2019JA027546.	2.4	13
28	Globalâ€Scale Observations and Modeling of Farâ€Ultraviolet Airglow During Twilight. Journal of Geophysical Research: Space Physics, 2020, 125, e2019JA027645.	2.4	16
29	Globalâ€Scale Observations of the Limb and Disk Mission Implementation: 1. Instrument Design and Early Flight Performance. Journal of Geophysical Research: Space Physics, 2020, 125, e2020JA027797.	2.4	14
30	Initial Observations by the GOLD Mission. Journal of Geophysical Research: Space Physics, 2020, 125, e2020JA027823.	2.4	80
31	Global‣cale Observations of the Equatorial Ionization Anomaly. Geophysical Research Letters, 2019, 46, 9318-9326.	4.0	76
32	Atmospheric Tides at High Latitudes in the Martian Upper Atmosphere Observed by MAVEN and MRO. Journal of Geophysical Research: Space Physics, 2019, 124, 2943-2953.	2.4	24
33	UV Study of the Fourth Positive Band System of CO and O <scp>i</scp> 135.6Ânm From Electron Impact on CO and CO ₂ . Journal of Geophysical Research: Space Physics, 2019, 124, 2954-2977.	2.4	12
34	Venus Upper Clouds and the UV Absorber From MESSENGER/MASCS Observations. Journal of Geophysical Research E: Planets, 2018, 123, 145-162.	3.6	41
35	Magnesium II Index measurements from SORCE SOLSTICE and GOES-16 EUVS. Proceedings of the International Astronomical Union, 2018, 13, 167-168.	0.0	1
36	Mars H Escape Rates Derived From MAVEN/IUVS Lyman Alpha Brightness Measurements and Their Dependence on Model Assumptions. Journal of Geophysical Research E: Planets, 2018, 123, 2192-2210.	3.6	42

#	Article	IF	CITATIONS
37	Observations of Mercury's Exosphere: Composition and Structure. , 2018, , 371-406.		5
38	Ultraviolet Solar Spectral Irradiance Variation on Solar Cycle Timescales. Proceedings of the International Astronomical Union, 2018, 13, 203-208.	0.0	3
39	Global Aurora on Mars During the September 2017 Space Weather Event. Geophysical Research Letters, 2018, 45, 7391-7398.	4.0	44
40	Evidence Connecting Mercury's Magnesium Exosphere to Its Magnesiumâ€Rich Surface Terrane. Geophysical Research Letters, 2018, 45, 6790-6797.	4.0	21
41	Discovery of a proton aurora at Mars. Nature Astronomy, 2018, 2, 802-807.	10.1	50
42	Significant Space Weather Impact on the Escape of Hydrogen From Mars. Geophysical Research Letters, 2018, 45, 8844-8852.	4.0	29
43	Martian Thermospheric Response to an X8.2 Solar Flare on 10 September 2017 as Seen by MAVEN/IUVS. Geophysical Research Letters, 2018, 45, 7312-7319.	4.0	24
44	Variability of D and H in the Martian upper atmosphere observed with the MAVEN IUVS echelle channel. Journal of Geophysical Research: Space Physics, 2017, 122, 2336-2344.	2.4	64
45	Martian mesospheric cloud observations by IUVS on MAVEN: Thermal tides coupled to the upper atmosphere. Geophysical Research Letters, 2017, 44, 4709-4715.	4.0	23
46	Detection of a persistent meteoric metal layer in the Martian atmosphere. Nature Geoscience, 2017, 10, 401-404.	12.9	52
47	Nitric oxide nightglow and Martian mesospheric circulation from MAVEN/IUVS observations and LMDâ€MGCM predictions. Journal of Geophysical Research: Space Physics, 2017, 122, 5782-5797.	2.4	36
48	IUVS echelleâ€mode observations of interplanetary hydrogen: Standard for calibration and reference for cavity variations between Earth and Mars during MAVEN cruise. Journal of Geophysical Research: Space Physics, 2017, 122, 2089-2105.	2.4	16
49	The Global-Scale Observations of the Limb and Disk (GOLD) Mission. Space Science Reviews, 2017, 212, 383-408.	8.1	105
50	Seasonal variations of Mercury's magnesium dayside exosphere from MESSENGER observations. Icarus, 2017, 281, 46-54.	2.5	38
51	Electron impact study of the 100ÂeV emission cross section and lifetime of the Lymanâ€Birgeâ€Hopfield band system of N ₂ : Direct excitation and cascade. Journal of Geophysical Research: Space Physics, 2017, 122, 6776-6790.	2.4	7
52	Simultaneous observations of atmospheric tides from combined in situ and remote observations at Mars from the MAVEN spacecraft. Journal of Geophysical Research E: Planets, 2016, 121, 594-607.	3.6	48
53	New discoveries from MESSENGER and insights into Mercury's exosphere. Geophysical Research Letters, 2016, 43, 11,545.	4.0	26
54	A coldâ€pole enhancement in Mercury's sodium exosphere. Geophysical Research Letters, 2016, 43, 12111-11128.	4.0	32

#	Article	IF	CITATIONS
55	Comparison of the Martian thermospheric density and temperature from IUVS/MAVEN data and general circulation modeling. Geophysical Research Letters, 2016, 43, 3095-3104.	4.0	34
56	Ultraviolet observations of the hydrogen coma of comet C/2013 A1 (Siding Spring) by MAVEN/IUVS. Geophysical Research Letters, 2015, 42, 8803-8809.	4.0	11
57	MAVEN IUVS observations of the aftermath of the Comet Siding Spring meteor shower on Mars. Geophysical Research Letters, 2015, 42, 4755-4761.	4.0	56
58	Nonmigrating tides in the Martian atmosphere as observed by MAVEN IUVS. Geophysical Research Letters, 2015, 42, 9057-9063.	4.0	43
59	Retrieval of CO ₂ and N ₂ in the Martian thermosphere using dayglow observations by IUVS on MAVEN. Geophysical Research Letters, 2015, 42, 9040-9049.	4.0	43
60	The structure and variability of Mars upper atmosphere as seen in MAVEN/IUVS dayglow observations. Geophysical Research Letters, 2015, 42, 9023-9030.	4.0	95
61	Threeâ€dimensional structure in the Mars H corona revealed by IUVS on MAVEN. Geophysical Research Letters, 2015, 42, 9001-9008.	4.0	67
62	MAVEN IUVS observation of the hot oxygen corona at Mars. Geophysical Research Letters, 2015, 42, 9009-9014.	4.0	77
63	Improving solar wind modeling at Mercury: Incorporating transient solar phenomena into the WSAâ€ENLIL model with the Cone extension. Journal of Geophysical Research: Space Physics, 2015, 120, 5667-5685.	2.4	16
64	New observations of molecular nitrogen in the Martian upper atmosphere by IUVS on MAVEN. Geophysical Research Letters, 2015, 42, 9050-9056.	4.0	41
65	A comparison of 3â€D model predictions of Mars' oxygen corona with early MAVEN IUVS observations. Geophysical Research Letters, 2015, 42, 9015-9022.	4.0	35
66	Probing the Martian atmosphere with MAVEN/IUVS stellar occultations. Geophysical Research Letters, 2015, 42, 9064-9070.	4.0	42
67	Neutral density response to solar flares at Mars. Geophysical Research Letters, 2015, 42, 8986-8992.	4.0	33
68	The Imaging Ultraviolet Spectrograph (IUVS) for the MAVEN Mission. Space Science Reviews, 2015, 195, 75-124.	8.1	139
69	The Mars Atmosphere and Volatile Evolution (MAVEN) Mission. Space Science Reviews, 2015, 195, 3-48.	8.1	563
70	MAVEN observations of the response of Mars to an interplanetary coronal mass ejection. Science, 2015, 350, aad0210.	12.6	166
71	Discovery of diffuse aurora on Mars. Science, 2015, 350, aad0313.	12.6	98
72	Early MAVEN Deep Dip campaign reveals thermosphere and ionosphere variability. Science, 2015, 350, aad0459.	12.6	90

#	Article	IF	CITATIONS
73	Mercury's seasonal sodium exosphere: MESSENGER orbital observations. Icarus, 2015, 248, 547-559.	2.5	74
74	Visible to near-infrared hyperspectral measurements of mercury: Challenges for deciphering surface mineralogy. , 2014, , .		2
75	Seasonal variations in Mercury's dayside calcium exosphere. Icarus, 2014, 238, 51-58.	2.5	60
76	The low-iron, reduced surface of Mercury as seen in spectral reflectance by MESSENGER. Icarus, 2014, 228, 364-374.	2.5	82
77	Mercury's Weather-Beaten Surface: Understanding Mercury in the Context of Lunar and Asteroidal Space Weathering Studies. Space Science Reviews, 2014, 181, 121-214.	8.1	108
78	Hydrogen atoms in the inner heliosphere: SWANâ€SOHO and MASCSâ€MESSENGER observations. Journal of Geophysical Research: Space Physics, 2014, 119, 8017-8029.	2.4	6
79	Global inventory and characterization of pyroclastic deposits on Mercury: New insights into pyroclastic activity from MESSENGER orbital data. Journal of Geophysical Research E: Planets, 2014, 119, 635-658.	3.6	79
80	Solar wind forcing at Mercury: WSAâ€ENLIL model results. Journal of Geophysical Research: Space Physics, 2013, 118, 45-57.	2.4	46
81	Lyman-Î \pm Models for LRO LAMP from MESSENGER MASCS and SOHO SWAN Data. , 2013, , 163-175.		6
82	A New Catalog of Ultraviolet Stellar Spectra for Calibration. , 2013, , 191-226.		23
83	Cassini UVIS observations of Titan nightglow spectra. Journal of Geophysical Research, 2012, 117, .	3.3	28
84	Modeling MESSENGER observations of calcium in Mercury's exosphere. Journal of Geophysical Research, 2012, 117, .	3.3	28
85	The production of Titan's ultraviolet nitrogen airglow. Journal of Geophysical Research, 2011, 116, .	3.3	49
86	Electron transport and precipitation at Mercury during the MESSENGER flybys: Implications for electron-stimulated desorption. Planetary and Space Science, 2011, 59, 2026-2036.	1.7	30
87	Limits to Mercury's magnesium exosphere from MESSENGER second flyby observations. Planetary and Space Science, 2011, 59, 1992-2003.	1.7	36
88	Constraints on Mercury's Na exosphere: Combined MESSENGER and ground-based data. Icarus, 2011, 211, 21-36.	2.5	32
89	Observations of metallic species in Mercury's exosphere. Icarus, 2010, 209, 75-87.	2.5	31
90	Monte Carlo modeling of sodium in Mercury's exosphere during the first two MESSENGER flybys. Icarus, 2010, 209, 63-74.	2.5	51

#	Article	IF	CITATIONS
91	The SORCE SIM Solar Spectrum: ComparisonÂwithÂRecentÂObservations. Solar Physics, 2010, 263, 3-24.	2.5	77
92	A comparison of the ultraviolet to near-infrared spectral properties of Mercury and the Moon as observed by MESSENGER. Icarus, 2010, 209, 179-194.	2.5	26
93	Mercury's Complex Exosphere: Results from MESSENGER's Third Flyby. Science, 2010, 329, 672-675.	12.6	70
94	Solar Irradiance Reference Spectra (SIRS) for the 2008 Whole Heliosphere Interval (WHI). Geophysical Research Letters, 2009, 36, .	4.0	171
95	EUVS-C: the measurement of the magnesium II index for GOES-R EXIS. , 2009, , .		6
96	MESSENGER Observations of Mercury's Exosphere: Detection of Magnesium and Distribution of Constituents. Science, 2009, 324, 610-613.	12.6	83
97	Titan airglow spectra from the Cassini Ultraviolet Imaging Spectrograph: FUV disk analysis. Geophysical Research Letters, 2008, 35, .	4.0	62
98	Mercury's Exosphere: Observations During MESSENGER's First Mercury Flyby. Science, 2008, 321, 92-94.	12.6	77
99	Spectroscopic Observations of Mercury's Surface Reflectance During MESSENGER's First Mercury Flyby. Science, 2008, 321, 62-65.	12.6	94
100	Radiation transport of heliospheric Lyman- <i>α</i> from combined Cassini and Voyager data sets. Astronomy and Astrophysics, 2008, 491, 21-28.	5.1	42
101	Titan airglow spectra from Cassini Ultraviolet Imaging Spectrograph (UVIS): EUV analysis. Geophysical Research Letters, 2007, 34, .	4.0	69
102	Mercury's Atmosphere: A Surface-Bounded Exosphere. Space Science Reviews, 2007, 131, 161-186.	8.1	47
103	The Geology of Mercury: The View Prior to the MESSENGER Mission. Space Science Reviews, 2007, 131, 41-84.	8.1	31
104	The Mercury Atmospheric and Surface Composition Spectrometer for the MESSENGER Mission. Space Science Reviews, 2007, 131, 481-521.	8.1	128
105	SORCE solar UV irradiance results. Advances in Space Research, 2006, 37, 201-208.	2.6	46
106	High time cadence solar Magnesium II index monitor. , 2005, 5901, 354.		4
107	Solar–Stellar Irradiance Comparison Experiment II (SOLSTICE II): Pre-Launch and On-Orbit Calibrations. Solar Physics, 2005, 230, 259-294.	2.5	73
108	The Mg II Index from SORCE. Solar Physics, 2005, 230, 325-344.	2.5	54

#	Article	IF	CITATIONS
109	Solar–Stellar Irradiance Comparison Experiment II (Solstice II): Instrument Concept and Design. Solar Physics, 2005, 230, 225-258.	2.5	150
110	Solar–Stellar Irradiance Comparison Experiment II (Solstice II): Examination of the Solar–Stellar Comparison Technique. Solar Physics, 2005, 230, 295-324.	2.5	68
111	The Cassini Ultraviolet Imaging Spectrograph Investigation. Space Science Reviews, 2004, 115, 299-361.	8.1	210
112	Solar irradiance variability during the October 2003 solar storm period. Geophysical Research Letters, 2004, 31, n/a-n/a.	4.0	166
113	Emission cross section of O I (135.6 nm) at 100 eV resulting from electron-impact dissociative excitation of O2. Geophysical Research Letters, 2001, 28, 1379-1382.	4.0	16
114	Galileo ultraviolet spectrometer observations of atomic hydrogen in the atmosphere of Ganymede. Geophysical Research Letters, 1997, 24, 2147-2150.	4.0	76
115	Latitude variations in interplanetary Lyman-α data from the Galileo EUVS modeled with solar He 1083 nm images. Geophysical Research Letters, 1996, 23, 1893-1896.	4.0	30
116	Direct observations of the comet Shoemaker-Levy 9 fragment G impact by Galileo UVS. Geophysical Research Letters, 1995, 22, 1565-1568.	4.0	16
117	Simple ultraviolet calibration source with reference spectra and its use with the Galileo orbiter ultraviolet spectrometer. Applied Optics, 1988, 27, 890.	2.1	84
118	Global-Scale Observations of the Limb and Disk (Gold): New Observing Capabilities for the Ionosphere-Thermosphere. Geophysical Monograph Series, 0, , 319-326.	0.1	8